

# Interpenetrating Network Formation in Gellan–Maltodextrin Gel Composites

A. H. Clark,\* S. C. E. Eyre, and D. P. Ferdinando

Unilever Research Laboratory, Colworth House, Sharnbrook, Bedford, MK44 1LQ, UK

S. Lagarrigue

E.S.P.C.I., 10, Rue Vauquelin, 75231 Paris Cedex 05, France

Received May 4, 1999

**ABSTRACT:** Formation of cold-set gels from mixtures of the bacterial polysaccharide gellan and the modified potato starch Paselli SA2 has been studied by mechanical spectroscopy, turbidity measurements, and confocal and transmission electron microscopy. The hot solutions gave no indication of a tendency to liquid–liquid demix over normal concentration ranges. A microphase-separated gel structure arose after a substantial period at 4 °C, but electron microscope evidence suggested aggregation of the starch polymers in a fine-pored homogeneous preformed gellan network, not simple separation of the two components into distinct gel phases. A novel method based on assessing local effective polymer concentrations during gelling, from mechanical cure curves and turbidity data, also suggested that a simple phase-separated microstructure was inappropriate, and an interpenetrating network model was able to describe shear modulus–composition data for the final gels.

## Introduction

Mixed biopolymer gels based on two polymer components and a solvent (usually water or a simple salt solution) have received considerable research interest<sup>1</sup> during the past decade mainly because of their role in foods and related soft solid materials. Such gels are normally formed from starting solutions by thermal quenching, often in the direction of high-to-low temperature, but not exclusively so. In practical applications, such quenching is conducted at a finite, and not necessarily extremely rapid, rate, but rapid and multiple stage quenching are possible. Options<sup>2</sup> for the hot solution include homogeneous solutions prepared outside the binodal and the more common situation of preparing water-in-water emulsions within the phase boundary. Important physical properties of the gels include elastic moduli, nonlinear stress–strain behavior and ultimate properties, and the thermal dependencies of these properties.

When dealing with such gels, and the processes that give rise to them, it is important to relate properties to microstructure and to understand the origins of the latter in terms of thermal and mechanical history. To date, however, only limited progress has been made. Gels of this kind generally have complex multiphasic microstructures and represent kinetically trapped states whose exact properties are history dependent. Early models<sup>3,4</sup> considered only final linear elastic properties and related these to phase-separated microstructure on the assumptions of total polymer segregation and a very simple relationship between modulus and the mechanical properties of the two polymer-rich phases involved. This approach followed very much the lead set by workers studying synthetic polymer blends,<sup>5</sup> but there was the additional element, not usually involved in that field, of a solvent present in very large amount. This meant that phase separation, even when it implied total polymer segregation, included solvent partition between the phases, the real polymer concentrations in the latter

being substantially different from their original nominal values. These modified values must be known if individual phase contributions to the entire material behavior are to be calculated.

An early way<sup>4</sup> of dealing with this situation was to assume that any pair of polymers, when becoming fully segregated, shared the solvent between them, not just according to their mass ratio, but this ratio multiplied by an empirical factor  $p$ . This parameter allowed for any bias, having its origins in an intrinsic tendency for one polymer to attract solvent more strongly than the other. At the time,  $p$  was regarded as dependent only on the two polymer types, and not on the amounts present, and somehow reflected relative hydrophilicity (where the solvent was water). It is evident in retrospect, however, that solvent partition in this way is very much a manifestation of the ternary solution behavior of a two-polymer–one solvent system and should be describable by such theories as that of Flory and Huggins.<sup>6</sup> As will be mentioned in more detail in the Theory section,  $p$  is very nearly equal to the tie line slope in phase diagrams, and this in turn is usually determined by the difference between polymer–solvent  $\chi$  values (though for polyelectrolyte mixtures the influence of dissociable counterions is also felt<sup>7</sup>).

Provided total segregation occurs (a condition determined by polymer–solvent and polymer–polymer  $\chi$  values and to some extent by the polymer molecular weights)  $p$  is very nearly constant over substantial regions of a ternary phase diagram and has a rigorous meaning. It is then possible to describe the ternary phase behavior in terms of  $p$  alone, and hence to relate phase volume fractions and the concentrations of components within these phases, to a single parameter. Elastic moduli are then calculable as isostress/isostain bounds based on the volume fractions of the separate phases and their individual concentration-dependent moduli.<sup>4</sup> Tests of such ideas against experiment have been performed for many polymer pairs, and success has been claimed.<sup>1</sup>

The above is a simplistic and rather limited approach to mixed biopolymer gels, however, and as more systems have been examined, and data accrued, it has become clear that more sophisticated models are necessary. In practice, complete polymer segregation between the phases of a gelling ternary solution is rarely achieved, and microstructures show subtleties beyond just a simple two-phase morphology (e.g., gelled inclusions formed by secondary demixing often occur within phases<sup>8</sup>). The simple additivity laws neglect such complications, focusing as they do purely on phase volumes, and ideas of a well-defined supporting and included phase. Interfacial surface effects are also neglected, and certain scenarios are omitted altogether, such as when simple macroscopic phase separation fails to occur, and the composite is based on trapped microphases, and/or the interpenetration of molecular networks (IPN's). Such complexity is to be expected in relation to the real phase behavior of ternary systems which allows incomplete segregation of polymers (tie lines of limited extent) and substantial regions of polymer compatibility (outside the binodal) from which intimately mixed structures can form (rapid gelling).

The present paper shows the need for studies of mixed biopolymer gelation to move in such newer directions, by considering a biopolymer mixture (charged gellan, uncharged Paselli SA2 modified starch, water) which resists demixing on quenching (counterion effect<sup>7</sup>) and gels rapidly through fast network building by the gellan component. Although preliminary mechanical measurements suggest that the conventional phase-separated segregated model should apply to this system, this is shown to be false both through microscopical studies of the gel microstructures and through a more critical evaluation of the phase-separated gel model's ability to describe cure curve data. Consideration is given to the problem of building a more appropriate model for the gel type involved, but it is concluded that this is a formidable task as the simple reference to pure component behavior, and the simple additivity laws for component contributions, which the elementary gel model offers, disappear for the more complex microstructures found here.

Gellan is an extracellular polysaccharide produced by the bacterium *Sphingomonas* (sometimes *Pseudomonas*) *elodea*.<sup>9</sup> It is a linear anionic heteropolysaccharide based on a tetrasaccharide repeat unit of glucose, glucuronic acid, and rhamnose. It forms cold-set, and often fairly transparent, gels in a manner similar to carrageenans, i.e., by initial formation of double-helical aggregates which associate to form fibrous three-dimensional networks. Paselli SA2,<sup>10</sup> on the other hand, derives from native potato starch through enzyme hydrolysis, during which both branched amylopectin and linear amylose suffer large reductions in molecular weight. Cold-set gels form by co-crystallization of branched amylopectin polymers with short linear amylose fragments to produce colloidal aggregates, which form the basis of a microphase-separated gel network and highly opaque gels. Molecular weight information is available for these polymers but was not required in the present work.

## Theory

The original theory<sup>3,4</sup> of segregated phase-separated composite gel formation is now examined in more detail, it being assumed to apply either to gels formed by quenching water-in-water emulsions already involving

total segregation or to those that achieve such segregation during the gelling process. The latter situation implies that during temperature change aggregation processes and temperature-induced changes in  $\chi$  values drive more complete demixing prior to gelation.

The original theory considered a starting solution containing mass fractions of solvent (component 1), polymer 2, and polymer 3, equal to  $m_1, m_2$ , and  $m_3$  ( $m_1 + m_2 + m_3 = 1$ ). In the fully segregated gel finally formed, it was assumed that a fraction of the solvent equal to  $\alpha m_1$  was added to the total mass of polymer 2 in a segregated phase A. Correspondingly, the remaining  $(1 - \alpha)m_1$  of the solvent combined with polymer 3 in phase B. This gave rise to final compositions for the two phases defined in terms of solvent and polymer mass fractions ( $m_1', m_2'$ ) for phase A and ( $m_1'', m_3''$ ) for phase B (note: through segregation  $m_3' = 0, m_2'' = 0$ ). Clearly, in terms of the initial solution composition,

$$m_1' = \alpha m_1 / (\alpha m_1 + m_2) \quad (1)$$

and

$$m_1'' = (1 - \alpha)m_1 / \{(1 - \alpha)m_1 + m_3\} \quad (2)$$

If water was simply partitioned according to the relative masses of the polymers present,  $\alpha/(1 - \alpha) = m_2/m_3$ , but to allow for a nonequivalence of interaction with solvent, the original model defined  $p$  (an "avidity" parameter) by the relationship

$$\alpha/(1 - \alpha) = p(m_2/m_3) \quad (3)$$

or

$$\alpha = pm_2 / (pm_2 + m_3) \quad (4)$$

Evidently when  $p$  is greater than unity, polymer 2 attracts solvent more strongly than 3, and vice versa for  $p$  less than one. By rearrangement of 1 to 4, and using the definition of mass fractions,  $p$  is given by

$$p = (m_3''/m_2')(m_1'/m_1'') \quad (5)$$

and since, for the case of total segregation of polymers, tie lines completely span the phase diagram, and no miscibility region is involved, it is clear that  $p$  is closely related to tie line slope (negative of first term in parentheses in eq 5, for a rectangular representation showing polymer concentrations on the axes). Thus,  $p$  is constant along any given tie line but could vary from tie line to tie line if (a) tie line slopes vary and/or (b) the second term in (5) varies. Over restricted ranges of concentrations, variations from these sources are expected to be small, giving some justification for the original approximation that  $p$  is dependent only on polymer type and not on solution composition. In effect, in this approximation, a completely segregated system, showing parallel tie lines, is fully defined by a single parameter  $p$ . Also, since it can be shown that tie line slope is a function of the difference in polymer-solvent  $\chi$  values ( $\chi_{12}$  and  $\chi_{13}$ ) specified by the Flory-Huggins theory<sup>6</sup> of polymer solutions, it is evident that  $p$  has a fundamental significance when considered in terms of these parameters. Unfortunately, an explicit analytical form for this relationship has so far evaded the present authors, but the truth of the assertion can be demonstrated by numerical computation. The Flory-Huggins

theory warns, however, that the extreme segregation assumed will only occur for certain values of polymer–solvent and polymer–polymer  $\chi$  values (and molecular weights) and that the more common situation for starting solutions is likely to be one of partial miscibility, with many tie lines failing to extend to the concentration axes. In such a situation  $p$  has no meaning and is not a useful concept, though one must remember that in many cases when gelling occurs from an incompletely demixed system segregation may become effectively complete, i.e., be promoted by the gelling event. This, in fact, is a reason sometimes given for the success of the model in situations where the pregelling solution state is known to be far from totally demixed.

In terms of  $p$ , and the initial polymer compositions  $m_2$  and  $m_3$ , the polymer mass fractions in phases A and B can be written as

$$m_2' = (pm_2 + m_3)/(p + (1 - p)m_3) \quad (6)$$

and

$$m_3'' = (pm_2 + m_3)/(1 - (1 - p)m_2) \quad (7)$$

and similar expressions can be produced for the volume fractions of the phases<sup>4</sup> if it is assumed that densities are approximately unity (or the transformation from mass to volume is made through partial specific volumes). It is useful to rewrite eqs 6 and 7 as series expansions in  $m_2$  and  $m_3$  as these reveal more of the underlying relationships involved and are easier to compare with other expressions to be derived later. These are

$$m_2' = m_2 + \{1 + (p-1)m_2\} \sum \{(p-1)^{n-1}/p^n\} m_3^n \quad (8)$$

and

$$m_3'' = m_3 + \{1 + (1/p - 1)m_3\} \sum \{p(1 - p)^{n-1}\} m_2^n \quad (9)$$

where  $n$  runs from 1 to infinity. They indicate that, if the effective polymer mass fraction in a phase is plotted against varying nominal concentration of the other polymer (at constant value of its own nominal concentration), an increasing power series is involved. If, on the other hand, the plot involves effective concentration of a component against its own nominal concentration (fixed concentration of the other polymer), linear expressions are obtained of the form

$$m_2' = \{1 + \sum \{(p-1)^n/p^n\} m_3^n\} m_2 + \sum \{(p-1)^{n-1}/p^n\} m_3^n \quad (10)$$

and

$$m_3'' = \{1 + \sum \{(1 - p)^n\} m_2^n\} m_3 + \sum \{p(1 - p)^{n-1}\} m_2^n \quad (11)$$

where, perhaps surprisingly, the values of  $m_2'$  and  $m_3''$  are finite when  $m_2$  and  $m_3$  are zero. This arises from the fact that, in the limit, as a given component falls in concentration at constant value of the other, the volume fraction of the phase rich in the polymer of interest tends to zero, while its effective concentration remains finite.

Expressions 6 and 7 form the basis of the present analysis of experimental data for the gellan–Paselli SA2

system. It should be emphasized that using the equations to fit effective vs nominal concentration data is quite novel as the more normal approach has been to measure final (fully set) composite gel moduli and fit these on the basis of a single  $p$  value and some assumption about additivity of the individual phase moduli. In this approach no direct measurement of phase volumes or effective concentrations is necessarily involved. These are predictions of the calculation not often verified in practice. In the present work, by contrast, attention focuses on ways of inferring values for the effective concentrations from the time dependence of modulus change during composite formation and from changes in other observables such as turbidity. These data are then fitted to obtain a  $p$  value and the implications for the final composite modulus tested by comparing predictions for this quantity. The success of the approach and the validity of a segregated and demixed description for the gels are then evaluated in terms of how good a prediction is made and, perhaps more particularly, how consistent  $p$  values are from plots involving the effective concentrations of the two separate polymer components. (For the model to be valid  $p$  should always have the same value irrespective of plot type.)

## Materials and Methods

**Materials.** Gellan was obtained in a mixed salt form from Kelco (Kelcogel F). The cation content of the gellan was 3.8% w/w potassium, 0.6% w/w sodium, and 0.2% w/w calcium. Paselli SA2 was a standard food grade material supplied by Avebe.

**Small-Deformation Rheology.** Gelling of samples was studied by small deformation oscillatory shear measurement using a Carrired CSL 500 stress-controlled rheometer. Parallel plate geometry was adopted (20 mm radius, 1 mm gap), and the plates were coated with 600 grade emery paper to minimize slippage. In preliminary experiments gellan/SA2 solutions were loaded hot (90 °C) onto the rheometer, with the bottom plate controlled at 5 °C and the system left for 15 h to setup with shear modulus components  $G'$  and  $G''$  being continuously monitored (stress 5 Pa, frequency 0.5 Hz). In more detailed work aimed at determining effective concentrations in phases, the bottom plate commenced at 90 °C, and the sample was cooled from 90 to 4 °C at 1 °C min<sup>-1</sup> before holding at this temperature for 13 h. As gelation commenced ( $G' = G''$ ) strain was controlled at 0.5% for pure polymer systems and 1% for mixtures. In all cases “melting” curves could be obtained by similar modulus measurement under conditions of scanned heating of the cured gels.

Solution preparation involved dissolving SA2 in deionized water at 95 °C for 15 min (vigorous stirring) followed by addition of the gellan. A further 20 min was required to complete dissolution, apparently homogeneous solutions always being obtained.

**Turbidity Measurements.** Turbidity measurements were made during the gelling of samples using a UV2101PC spectrophotometer at 800 nm. The path length was 1 cm, and deionized water was used as a standard. The temperatures of cuvettes were controlled to within 1 °C, and temperature profiles were matched as closely as possible to those used in the rheological experiments.

**Confocal Microscopy.** A slide and coverslip carrying hot gellan/SA2 solution was placed on the heated stage of a confocal microscope (90 °C) and a micrograph recorded. The solution was then cooled at a rate of 7 °C min<sup>-1</sup> to detect phase separation and a second micrograph recorded at 25 °C. A final micrograph was obtained after the sample had remained at 4 °C for 16 h. In some cases where gels were cured outside the instrument a section (size 10 × 10 × 3 mm) was cut and placed on a microscope slide, stained with iodine for starch, and

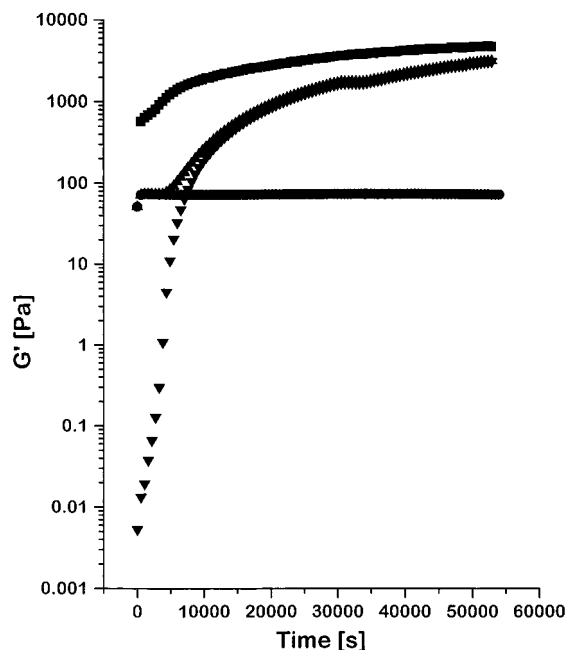


**Figure 1.** Cure curves (5 Pa, 0.5 Hz, 5 °C, 15 h) for (●) 1% w/w gellan, (▼) 20% w/w SA2, (▲) sum of 1% gellan and 20% SA2, (■) 1/20% w/w gellan/SA2 mixture.

covered with a coverslip. The confocal instrument used was a Board MRC 600 confocal scanning laser microscope with a laser excitation at 488 nm, and images were displayed at a depth of greater than 25  $\mu\text{m}$  using an oil immersion objective ( $60 \times 1.4 \text{ na}$ ).

**Transmission Electron Microscopy.** Samples of fully cured gel were cut into small cubes and fixed in 0.5% aqueous ruthenium tetroxide for 2 h, followed by rinsing in two changes of distilled water for 15 min each. Samples were then fixed in 1% aqueous uranyl acetate for 2 h, followed by rinsing in distilled water. They were then dehydrated through 70, 90, and  $3 \times 100\%$  alcohol and  $2 \times$  acetone for 30 min each. Samples were then left in a 50:50 mixture of acetone/TAAB resin for 24 h, transferred to 100% resin for 24 h, and finally embedded in 100% resin at 60 °C for 48 h. Sections were cut using an Ultracut E microtome and examined on a JEOL 100CXII transmission electron microscope.

## Results

**Cure Curve Studies.** The dynamic shear modulus during cure was monitored for cooled gellan/SA2 solutions as indicated in the Experimental Section. Preliminary results for a 1/20% w/w gellan/SA2 system are shown in Figure 1 and for a 3/20% w/w system in Figure 2. Results for the pure gellan and starch components at the same concentrations, and under the same cooling and heating conditions, are also shown. From the cure curves in Figures 1 and 2, it is clear that the gellan gel sets up extremely rapidly, both in the composite and in the pure form, and that, at 1% w/w, while its modulus is quite low when gelled alone, this low value is increased almost 10-fold in the mixture. It is also clear that simple additivity of the individual component moduli cannot reproduce the composite cure curve even approximately. While somewhat similar conclusions can be reached for the 3% gellan example, here the increase in the gellan gel strength on adding starch is less pronounced. Shear modulus–temperature “meltdown” data also obtained (but not shown here) revealed high melting character (greater than 80 °C) for both gel mixtures, but it was difficult to separate gellan and Paselli individual contributions and obtain further

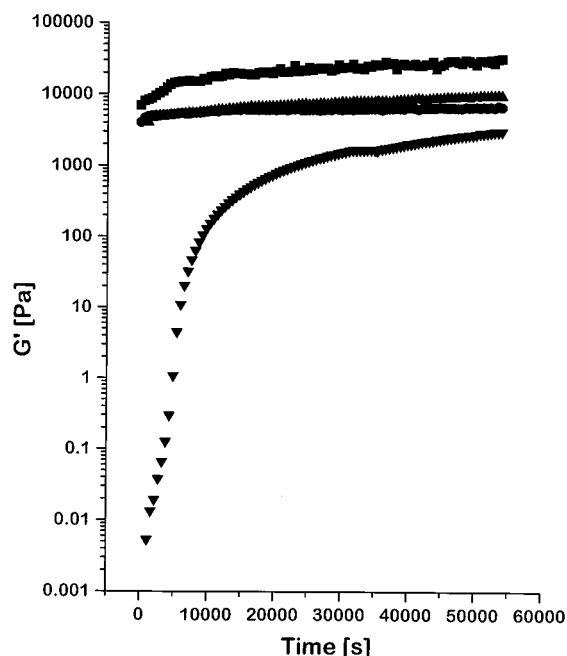


**Figure 2.** Cure curves (5 Pa, 0.5 Hz, 5 °C, 15 h) for (●) 3% w/w gellan; (▼) 20% w/w SA2; (▲) sum of 3% gellan and 20% SA2; (■) 3/20% w/w gellan/SA2 mixture.

information about gelling mechanism or microstructure. Superficially at least, the results obtained for both compositions could be consistent with a simple phase-separated microstructure, with segregation of the components.

To clarify the situation further, and to make a more quantitative analysis of the mechanical data in terms of the fully segregated model, it was decided to carry out additional cure experiments for three series of composite systems, i.e., systems based on three distinct nominal gellan concentrations (0.5% w/w, 1.5% w/w, and 2.5% w/w) and Paselli SA2 nominal concentrations of 5, 10, 15, 20, 25, and 30% w/w. Cure curves were measured for these compositions under slightly different, and more controlled, conditions of temperature scan and strain control (see the Experimental Section), and similar data were obtained for the pure components over a range of concentrations to provide reference values for gel times, gelation temperatures, and fully cured gel moduli. In addition, for both the composites and pure systems, turbidity was also monitored during the gelling processes, to indicate times at which turbidity began to rise rapidly, i.e., at which the starch began to aggregate. For the pure gellan and SA2, all of these data were available as plots against concentration, to allow interpolation, in exercises aimed at determining effective concentrations of the components in the gelling mixtures. These concentrations formed the basis of further calculations using the fully segregated gel description.

Before discussing the results of these tests, some further comment is necessary about effective concentration measurement. For a composite gel formed by segregative demixing, the effective concentration of a component in a phase determines the gelling characteristics of that phase and ultimately the contribution the phase makes to the overall composite behavior. It is clearly important to devise methods for measuring effective concentrations, as values for these, together with values for the volume fractions of the phases present, and a demonstration that such phases actually

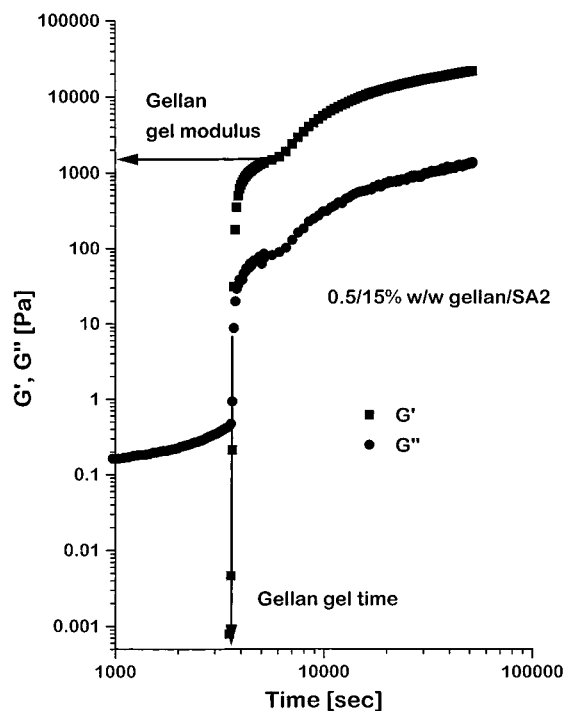


**Figure 3.** Cure curve for 0.5/15% w/w gellan/SA2 mixture showing the gel time feature used in assessing gellan effective concentration. For gelling conditions see text.

form, provide procedures for validating models describing overall composite properties. Of course, the models must not themselves be used at any stage to establish the concentrations, as circularity ensues.

Effective concentration measurement is, however, quite difficult and has not been widely reported or used in testing gel models. The most direct way would be spectroscopic determination applied microscopically to the individual composite phases, either in pregelling solutions or in gels, and some progress has been made in this direction using infrared<sup>11</sup> and Raman microscopes and confocal microscopy.<sup>12</sup> Where this is unavailable, however, methods have to rely on some concentration-dependent feature of the gelling process in a phase, which can be monitored during the gelling of the composite as a whole and attributed to the segregated component in that phase without ambiguity.

In the present work this is the approach adopted, it being argued that the effective concentration in any gellan-rich phase can be inferred by comparison of the initial part of the composite cure curve with that of pure gellan standards measured under the same temperature scan rate. The times (or temperatures) at which gelling just commences, and also when the gelation rate is at a maximum (Figure 3), should both be concentration-sensitive and serve as empirical indicators of concentration when calibrated against standards (provided, as is assumed here, that no significant changes in salt content accompany the addition of the second component).

For the later gelling SA2 component the situation is much more difficult as the corresponding rheological features are obscured by the gellan cure contribution or require some model assumption to deconvolute them from the experimental data. In consequence, in the present work, turbidity–time relationships, which are sensitive to the aggregation of SA2 alone, are used in a manner analogous to the cure curves, as such features

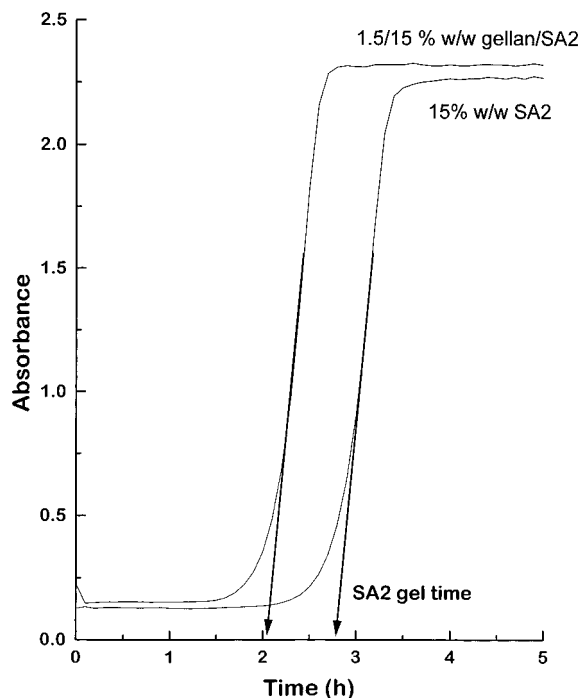


**Figure 4.** Light absorbance–time data for a gelling gellan/SA2 mixture and corresponding pure SA2, showing features used in assessing Paselli SA2 effective concentrations. For gelling conditions see text.

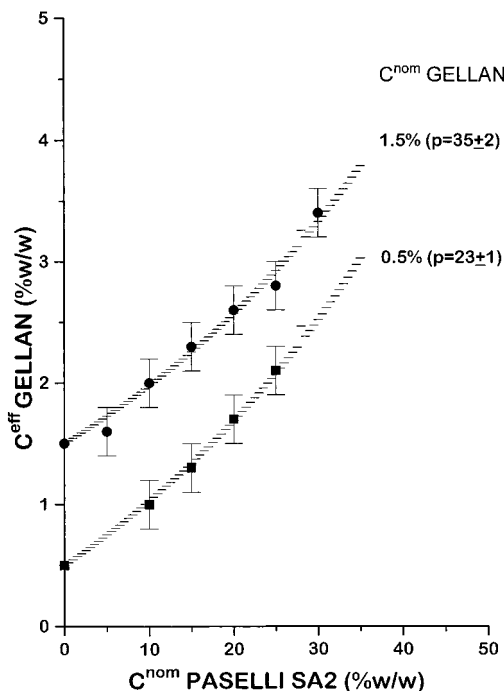


**Figure 5.** Gellan effective concentration data (0.5% and 1.5% w/w gellan series) expressed as a function of nominal Paselli SA2 concentration and fitted using fully segregated phase-separated model (eq 6).

(Figure 4) as the time (or temperature) of initial turbidity increase and the maximum rate of increase are also highly concentration-sensitive.

Average results for effective gellan concentrations (two methods above) and estimated error limits are plotted against nominal Paselli SA2 concentrations in Figure 5. Results for fixed nominal gellan concentrations of 0.5% and 1.5% w/w only are shown and include points at zero added SA2 where obviously the effective and

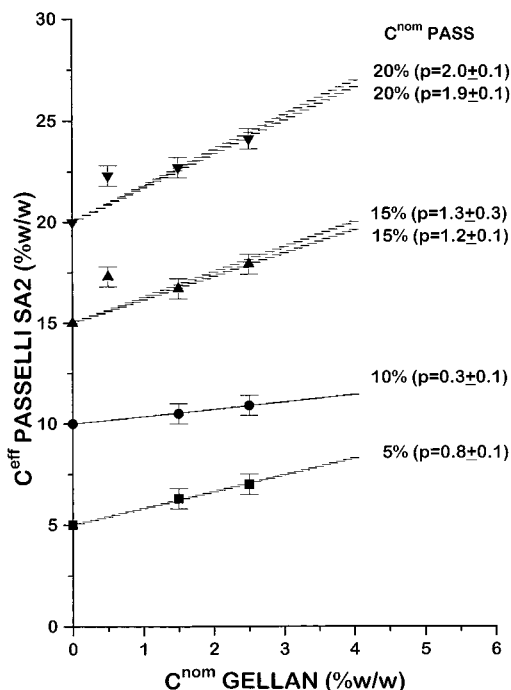


**Figure 6.** Paselli SA2 effective concentration data (0.5%, 1.5%, and 2.5% w/w gellan series) expressed as a function of nominal gellan concentration and fitted using fully segregated phase-separated model (eq 7). Fits including and excluding the 0.5% gellan data points are indicated.

nominal concentrations are equal. Cure curves for the 2.5% w/w gellan series were also measured but showed evidence of slippage, and poor reproducibility, and have been omitted. Interestingly, the effective gellan concentrations estimated were reasonably consistent with the first modulus plateaus in cure curves (see Figure 3) attributed to initial gellan network formation. These plateau values were not used in effective concentration measurement, however, as a model assumption would be required to subtract out any SA2 contribution (circularity problem mentioned above). This last was probably quite small at the initial plateau stage.

Broken lines show the results of fitting the data using eq 6 (constrained to pass exactly through the 0% SA2 points), the fit being with respect to the parameter  $p$  only, results for which are also indicated. The fits are good, and the high  $p$  values obtained (though somewhat different) both suggest relatively much higher hydrophilicity for the gellan than the SA2. The expectation would be that in any gellan/SA2 composite the starch would be greatly concentrated by the gellan. This result is consistent with existing information about the polymers (gellan charged and hydrophilic, and starch likely to have a Flory–Huggins  $\chi$  value close to 0.5).

A corresponding plot of effective SA2 concentration (average of two methods involving turbidity) versus nominal gellan concentration appears in Figure 6 for a series of fixed nominal SA2 concentrations (5, 10, 15, and 20% w/w). The gellan 2.5% w/w results have been included, as the SA2 effective concentrations were inferred from turbidity measurements, not cure curves. Fitting has again been performed with respect to  $p$ , in this case using eq 7 (with the 0% gellan constraint), both including two rather poor 0.5% gellan data points and omitting these. The answers for  $p$  are not much different between these two calculations, and overall, two observations can be made. First, the value of  $p$ , which should

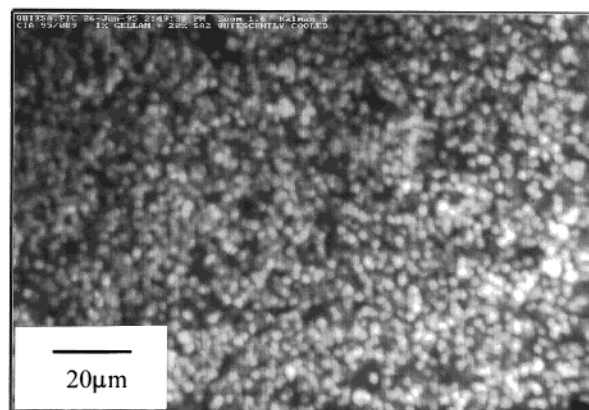


**Figure 7.** Confocal micrograph of a 1/20% w/w gellan/SA2 solution cooled to 4 °C and left for 13 h. A heterogeneous network structure can be seen based on SA2 micron-sized particles (lighter phase) distributed through a preformed gellan network (see text).

be the same as that determined from the effective gellan concentration data in Figure 5, is very different from the value between 20 and 30 obtained there; and second, apart from the rather low result obtained at 10% SA2, it is fairly consistent from one Paselli concentration to another. The overall low value of  $p$  found, if taken in isolation, would imply that the gellan and starch are of comparable hydrophilicity and that the starch would not be enormously concentrated in composites. In other words, when viewed from the starch point of view there is no evidence of this being highly concentrated in the presence of gellan when its gelling behavior is measured. To an approximation both polymers appear to occupy the full space of the system, which is impossible in a simple phase-separating system.

Clearly a very significant contradiction has been exposed, which implies that the fully segregated model is unsatisfactory as a description of gellan–SA2 composites. In the section that follows further evidence from microscopy supports this view by showing the absence in the gels of either fully or partially segregated structures.

**Microscopy of Gellan/SA2 Mixtures.** Hot (90 °C) gellan/SA2 mixtures, in the concentration ranges 0.4–3% w/w gellan and 2–20% w/w Paselli SA2, showed no obvious signs of phase separation on visual inspection, apart from what appeared to be the formation of very small amounts of a white precipitate. Centrifugation at 70 °C did not alter this conclusion, nor did examination under a confocal microscope. Thus, when a 1/20% w/w gellan/SA2 mixture was studied at 90 °C, using this instrument, no indication of liquid–liquid demixing was obtained.

Confocal microscopy was continued during cooling, examination being made of the states of the gellan/SA2 system on first reaching 25 °C and after 16 h at 4 °C. On reaching 25 °C, the gellan is expected to have gelled (previous mechanical spectroscopy), and if this has involved true segregation, clear evidence of demixing would be expected in confocal micrographs. These latter were indeed slightly different from high temperature versions, being mottled and clouded in appearance, rather than totally uniform, but no well-defined separation into two phases was suggested. Only after a substantial period at 4 °C (during which the gel became fully cured and opaque) was there definite evidence of distinct phases. As the confocal micrograph in Figure 7

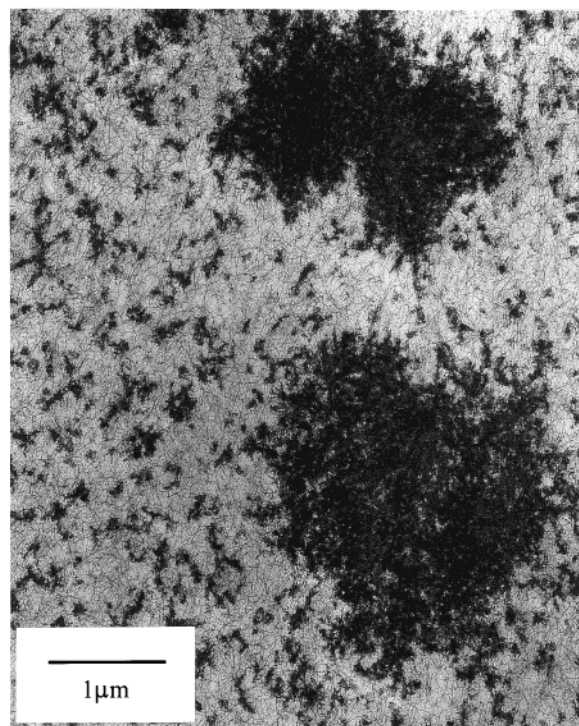


**Figure 8.** Transmission electron micrograph of a cooled, microphase-separated, 1.4/12% gellan/SA2 gel. Note that the gellan network appears to interpenetrate the SA2 particles, suggesting that these formed after the gellan network became complete.

shows, at this stage, a network of micron-sized particles has formed which, from staining, appears to be based on the Paselli component. The confocal image obtained is actually very similar to those observed for gels based on the pure SA2 component alone, this substance being well-known<sup>10</sup> to form gel networks based on small evenly sized semicrystalline starch aggregates. At this level of spatial resolution, the gellan has apparently had little influence on the phase character of the composite. It seems that even in the fully cured gel, although a form of phase separation has occurred involving crystallization of the starch, there is no evidence of a structure based on segregated gellan and SA2 gelled phases, if by the latter is meant a distinct volume of gel network formed from discrete SA2 particles.

Other mixture concentrations were examined within the ranges indicated above, and the same results found, confirming the visual and centrifugation observations and suggesting that solution homogeneity persists, certainly up to the gelling of the gellan and to some extent beyond. Real inhomogeneities only develop as the SA2 network forms, and this form of microstructure would be found even in the absence of gellan.

Further information about the gel microstructures was obtained using transmission electron microscopy. Figure 8 shows a high magnification view of a 1.5/12% w/w gellan/SA2 fully cured gel. The components can easily be identified in relation to micrographs for the pure gelling materials. Electron micrographs (not shown here) reveal the gellan network as fine meshed, based on rather uniform fine fibers and of small pore size, while the Paselli SA2 stains much darker and forms dense aggregates (Figure 9). In the pure material, these aggregates appear more solid and compact than in the composite, but they are of comparable size. Their size distribution may be more smoothly continuous, however,

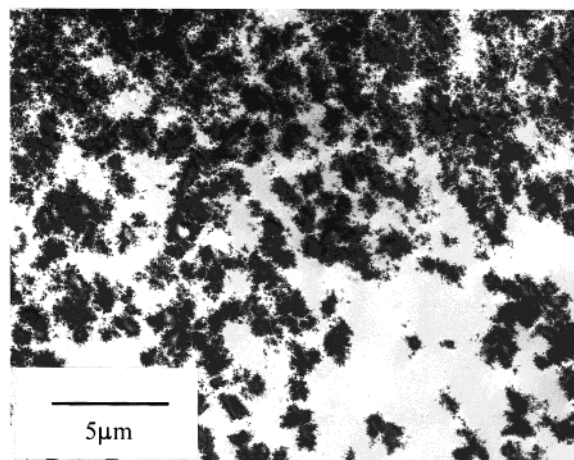


**Figure 9.** Transmission electron micrograph of a cooled 20% w/w SA2 solution for comparison with Figure 8.

for in the mixed gels, aggregates of micron size coexist with a population of very much smaller particles. Furthermore, for the composites, the large aggregates appear to be loose associations of these much smaller ones, leading to the apparent difference in compactness already noted. In fact, in relation to this, close examination of Figure 8 suggests that the gellan network may pass uniformly through the larger starch aggregates, though this is not absolutely proved. Such a picture would be consistent with the mechanical and optical micrograph evidence.

Interestingly, on lowering SA2 concentration, electron micrographs (not included here) show only the very small aggregates, and these are effectively invisible in corresponding confocal images. The heterogeneities observed by confocal microscopy for more concentrated systems (Figure 7, for example) appear to correspond to the largest clusters in Figure 8. Unfortunately, micrographs at high SA2 concentration are not so far available, but it is to be expected that the large clusters will greatly increase in number and percolate.

## Discussion

The experimental data from mechanical measurements and microscopy suggest that gellan/Paselli SA2 composites are unsuitable for description in terms of models directed toward phase-separated highly segregated systems. The composite gels do have phase-separated microstructures, but this is largely the result of the starch component crystallizing in the pores of a preformed gellan network. Normal SA2 gels are similarly (but not identically) phase separated in the absence of gellan, and this kind of inhomogeneity is not what is anticipated by the segregated model when it refers composite behavior to the gelling behavior of components. The most natural conclusion is that the resistance to demixing between gellan and SA2, caused by the polyelectrolyte character of the gellan and the absence of high ionic strength, means that gelling proceeds rapidly in a homogeneous solution (for the gellan) and that the starch later aggregates within the pores of this network. Such a result is probably best described as a molecularly interpenetrating network. This result simply emphasizes the fact that where gelling competes strongly with demixing and suppresses the latter, and particularly where the driving force for demixing is itself low (as for charged–uncharged systems), mixed biopoly-

mer gel microstructures can be obtained that differ substantially from the simple fully segregated picture.

If, as seems certain, the simple segregated gel model cannot be applied to systems of the present kind, there remains the task of finding a revised model that can still be used to link composite properties to the behaviors of the pure components. Where a component is not concentrated by phase separation, but still gels differently from expectation based on its nominal concentration, such a link will be hard to find, since the effect observed must be a consequence of changing gelling parameters such as cross-linking rates or affinities (reversible case), changes in the intrinsic strengths of gel network strands, or even the character of the gelling molecule (e.g., the number of cross-linking sites available).

Such an alteration in gelling character, rather than real physical segregation, appears to be the case for gellan/Paselli composites of the kind examined here, and in an attempt to deal with this situation, the following approach was tentatively explored. For a gelling system, past experience<sup>13–15</sup> has suggested that various measurable properties such as gel times, and other features of kinetic cure curves, including the modulus after long curing times, can be written in master curve form in terms of a reduced concentration  $C/C_0$ , where  $C_0$  is a critical concentration, dependent on molecular weight, number of cross-linking sites, and rate constants determining the course of cross-linking. If a polymer (2) is aggregating, and gelling, in a solution that contains significant amounts of another polymer component (3), and no segregation occurs, any change in gelling behavior most likely arises from a change in the parameters determining  $C_0$ , particularly the cross-linking rate constants (or a related equilibrium constant if cross-linking equilibrium is established). Thus, a change in critical concentration  $C_0$  to  $C_0'$  is to be expected in these circumstances. If the effect is not too large, the ratio  $C_0/C_0'$  for component (2) in the presence of varying amounts of (3) may be written as an expansion,

$$C_0/C_0' = 1 + k_1 m_3 + k_2 m_3^2 + \dots \quad (12)$$

where  $k_1$  and  $k_2$  (and higher values, if necessary) are empirical coefficients describing the intrinsic effect of component (3) on (2) and  $m_3$  is the nominal concentration of (3).

It is now proposed that, for convenience in analyzing data, the real change in critical concentration for a polymer component can be reinterpreted in terms of a corresponding fictitious change in its concentration (for example, for component (2), from nominal  $m_2$  to  $m_2'$ ), analogous to the real concentration effect occurring on segregation. This change is defined by the relationship

$$m_2'/C_0 = m_2/C_0'$$

or

$$m_2' = m_2(1 + k_1 m_3 + k_2 m_3^2 + \dots) \quad (13)$$

which defines  $m_2'$  to preserve the ratio  $C_0/C_0'$  and treats the system as if the gelling parameters had actually remained constant, while concentration had changed. This stratagem would seem necessary if reference is still to be made in a simple way to the gelling behavior of the pure components. Thus, if measurements are made of gel times, temperatures, turbidity onset times, etc.,

**Table 1. Gellan/SA2 Results: Fits to Effective Gellan Concentration vs Nominal Paselli SA2 Concentration Data (Figure 5) Using Eq 13<sup>a</sup>**

nominal gellan concn, % w/w	$k_1$	$k_2$
0.5	7.9 (0.5)	20 (2)
1.5	2.7 (1.0)	5 (3)
2.5		

<sup>a</sup> Esd's appear in parentheses. No results obtained at 2.5% gellan (see text).

**Table 2. SA2/Gellan Results: Fits to Effective Paselli SA2 Concentration vs Nominal Gellan Concentration Data (Figure 6) Using Eq 14**

nominal SA2 concn, % w/w	$q_1$	$q_2$
5.0	16.1 (0.9)	0 (fixed)
10.0	3.6 (0.2)	0 (fixed)
15.0	7.7 (0.1)	0 (fixed)
20.0	8.3 (0.5)	0 (fixed)

values for these "effective" concentrations can be obtained much as for true segregation, i.e., by methods such as those used here for the gellan/Paselli system. These will give values for  $m_2'$  and  $m_3'$ , where  $m_3'$  is given by a relationship analogous to (13), i.e.

$$m_3' = m_3(1 + q_1 m_2 + q_2 m_2^2 + \dots) \quad (14)$$

which, for the present gellan/Paselli example, would be interpreted as the influence of a gellan network on the gelling properties of the Paselli.

Thus, in cases where doubt attaches to the segregated description (as it does here), plots of  $m_2'$  vs  $m_3$ , and  $m_3'$  vs  $m_2$ , can be fitted using eqs 13 and 14 to obtain the series coefficients, particularly  $k_1$ ,  $k_2$  and  $q_1$ ,  $q_2$ . These coefficients will only prove useful if (a) higher order values are very small and (b) the values depend only on the identities of the polymers involved, not on their nominal amounts. The approach does, however, increase the number of parameters from one for the segregated model (one parameter  $p$ ) to at least two values,  $k_1$  and  $q_1$ , and probably more ( $k_2$ ,  $q_2$ ). This simply reflects the increased complexity of the IPN situation.

Interestingly, comparison of eqs 13 and 14 with eqs 8–11 shows that, while plots of  $m_2'$  vs  $m_3$  (fixed  $m_2$ ) and  $m_3'$  vs  $m_2$  (fixed  $m_3$ ) are series expansions, as in the segregated model case, plots of  $m_2'$  vs  $m_2$  (fixed  $m_3$ ) and  $m_3'$  vs  $m_3$  (fixed  $m_2$ ) are different, to the extent that they are straight lines through the origin (i.e., they do not have the finite limiting intercepts expected for the fully segregated approach). This last difference could present another way of discriminating the segregated case from others, but it may be quite hard to apply unless very substantial, and accurate, data are available. This approach will not be pursued here, but coefficient results of fitting eqs 13 and 14, in series fashion, to the data already presented in Figures 5 and 6, appear in Tables 1 and 2. Calculations varying the number of series terms included in expansions suggested that a quadratic term was necessary to describe the gellan effective concentration data, but only a linear term was required for the corresponding Paselli data. Addition of higher terms simply introduced larger uncertainties in coefficient values, and the additional terms were generally much smaller than their predecessors.

While truncation of the series seems reasonable, and the first criterion of success suggested above is therefore satisfied, the coefficients shown in Tables 1 and 2 are unfortunately not strongly consistent, as nominal con-

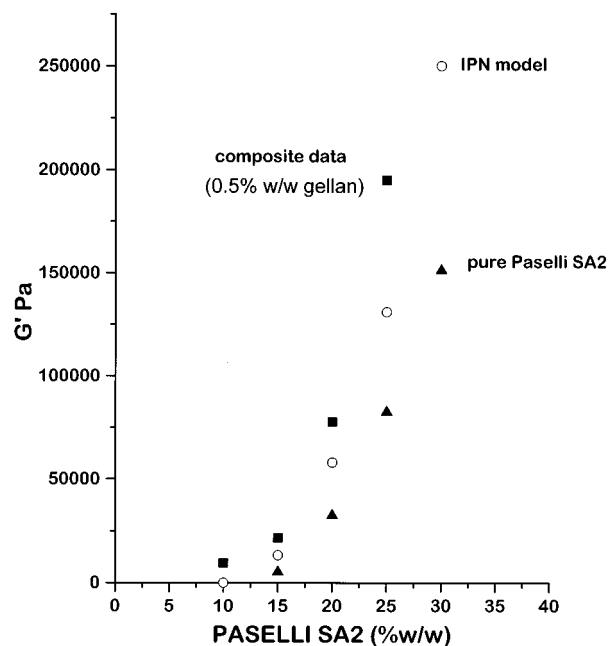


**Figure 10.** Shear modulus data for fully cured gellan/SA2 systems (0.5% w/w gellan series of samples) are compared with corresponding results for pure Paselli gels and with values calculated using effective concentration data and the IPN models of eqs 13 and 14. Note that the modulus of a pure 0.5% w/w gellan gel would be insignificant on the scale used here for  $G'$ .

centrations vary, so there is certainly real doubt about criterion two. This lack of consistency can in fact be demonstrated without recourse to curve fitting, by simply dividing the effective concentration data sets by the corresponding nominal concentrations and superposing results. Equations 13 and 14 suggest that these curves should overlay, irrespective of the mathematical form appropriate to the functions in parentheses. This property also distinguishes the new model from the old, as it would not be expected for a truly phase-separating system (see eqs 8 and 9). It is related to the intercept difference between the models highlighted earlier.

The interpenetrating network model can be assessed in other ways, too: for example, in relation to its ability to describe final moduli for the composites. This again can be done without reliance on a specific mathematical description of the effective concentration data. A reversal of the argument used to justify, and provide meaning, to such concentrations allows estimation of component contributions to the composite moduli, these being interpolated from modulus–concentration data for the pure systems. If it is then assumed that, to a first approximation, these contributions can simply be added together (as opposed to the phase volume and bounds approach appropriate to segregated systems), the results shown in Figures 10 and 11 are obtained. These show how the influence of gellan on SA2, and vice versa, can be modeled fairly well, though there is some underestimation of the composite moduli, which is likely to reflect the rather simplistic additivity law assumed here for the component networks. Increased sophistication in this last respect is clearly implicit in the new model and will inevitably have to be addressed.

The present work has shown how both microscopy and modeling of effective concentration data provide evidence that gelled gellan/Paselli SA2 mixtures cannot be regarded as simple phase-separated segregated com-

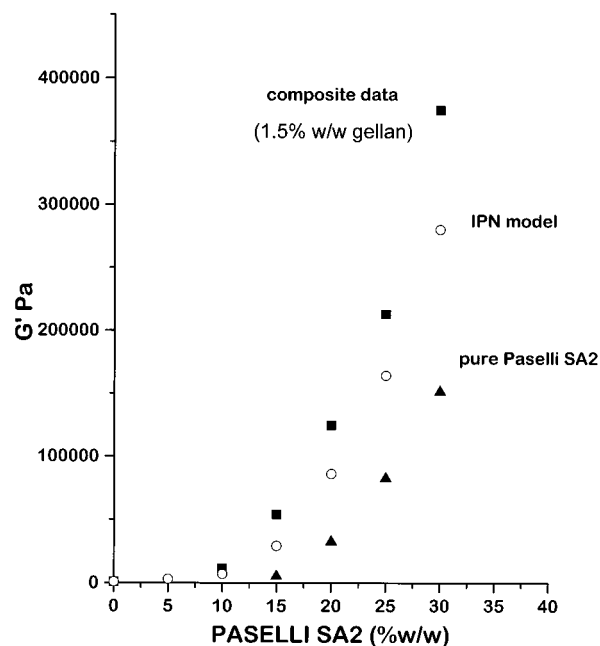


**Figure 11.** Similar results to those in Figure 10 but for constant 1.5% w/w gellan. Note that the modulus for a pure 1.5% w/w gellan gel would be insignificant on the scale used here for  $G'$ .

posite gels. The combination of a charged and uncharged biopolymer, at low ionic strength, inhibits demixing prior to gelation, and instead, gelation involves the building of an interpenetrating network structure. The second component is microphase separated if it is true, but this is a feature of the gelling starch component even on its own and should not be regarded as evidence of prior demixing. The mechanical behavior of the new type of network structure cannot be described by models developed for genuine phase separation of the two gelling components, in which real mutual concentration is assumed.

Where components form networks throughout the volume of the sample, and do not suffer physical concentration, the old segregative approach clearly fails. However, here it is argued that some elements of this approach can be retained, by reassigning changes in critical concentration, caused by changes in gelling parameters, to apparent changes in effective concentration. Composite behavior is then still related to data for the pure components. Some success is achieved, but this is qualified in terms of the lack of consistency of effective concentration data noted above, particularly for the 0.5% w/w gellan systems. In consequence, the generalization of the segregated model described here, which removes certain physical constraints involving solvent partition, but retains much of the methodology of the older approach, must be regarded as highly tentative and empirical, particularly as changes in  $C_0$  do not exert sole influence on changes in observable properties for gelling systems. The master plots appealed to, to justify this approach, usually involve vertical shifts in property variables (related to changes in the same parameters that influence the critical concentration), as well as concentration shifts, and this is difficult to incorporate rigorously into the new model. Where this effect is strong, reference of composite behavior to the behavior of pure systems may actually be impossible, and some other way of approaching the problem will be required.

**Acknowledgment.** The authors thank colleagues at the Colworth Laboratory for many helpful discussions and are particularly grateful to Mrs. J. E. Brigham for providing electron micrographs.

## References and Notes

- (1) *Biopolymer Mixtures*; Harding, S. E., Hill, S. E., Mitchell, J. R., Eds.; Nottingham University Press: Nottingham, 1995.
- (2) Clark, A. H. *Annu. Trans. Nordic Rheol. Soc.* **1998**, *6*, 19–26.
- (3) Clark, A. H.; Richardson, R. K.; Ross-Murphy, S. B.; Stubbs, J. M. *Macromolecules* **1983**, *16*, 1367–1374.
- (4) Clark, A. H. In *Food Structure and Behaviour*; Lillford, P. J., Blanshard, J. M. V., Eds.; Academic Press: London, 1987; pp 13–34.
- (5) *Polymer Blends and Composites*; Manson, J. A., Sperling, L. H., Eds.; Heyden Press: London, 1976.
- (6) Flory, P. J. *Principles of Polymer Chemistry*; Cornell University Press: Ithaca, NY, 1953.
- (7) Picullel, L.; Bergfeldt, K.; Nilsson, S. In *Biopolymer Mixtures*; Harding, S. E., Hill, S. E., Mitchell, J. R., Eds.; Nottingham University Press: Nottingham, 1995; pp 13–35.
- (8) Clark, A. H.; Richardson, R. K.; Robinson, G.; Ross-Murphy, S. B.; Weaver, A. C. *Prog. Food Nutr. Sci.* **1982**, *6*, 149–160.
- (9) Morris, V. J. In *Functional Properties of Food Macromolecules*, 2nd ed.; Hill, S. E., Ledward, D. A., Mitchell, J. R., Eds.; Aspen Publishers Inc.: Gaithersburg, MD, 1998; pp 188–195.
- (10) Kasapis, S.; Morris, E. R.; Norton, I. T.; Clark, A. H. *Carbohydr. Polym.* **1993**, *21*, 243–268.
- (11) Durrani, C. M.; Donald, A. M. *Carbohydr. Polym.* **1995**, *28*, 297–303.
- (12) Blonk, J. C. G.; Eendenburg, J. Van; Koning, M. M. G.; Weisenborn, P. C. M.; Winkel, C. *Carbohydr. Polym.* **1995**, *28*, 287–295.
- (13) Clark, A. H.; Ross-Murphy, S. B. *Br. Polym. J.* **1985**, *17*, 164–168.
- (14) Clark, A. H. *Polym. Networks* **1993**, *1*, 139–158.
- (15) Clark, A. H.; Farrer, D. B. *J. Rheol.* **1995**, *39*, 1429–1444.

MA990705P